

## Kurtosis of momentum and displacement distributions in biphenyl

P. ULPANI<sup>(1)</sup>, G. ROMANELLI<sup>(2)</sup>, D. ONORATI<sup>(3)</sup>, M. KRZYSTYNIAK<sup>(2)</sup>,  
C. ANDREANI<sup>(3)</sup><sup>(4)</sup> and R. SENESI<sup>(3)</sup><sup>(5)</sup><sup>(6)</sup>

<sup>(1)</sup> *Università degli Studi di Roma “Tor Vergata”, Dipartimento di Scienze e Tecnologie Chimiche - Via della Ricerca Scientifica 1, Rome, 00133 Italy*

<sup>(2)</sup> *ISIS Facility, Rutherford Appleton Laboratory - Chilton, Didcot, OX110QX, UK*

<sup>(3)</sup> *Università degli Studi di Roma “Tor Vergata”, Dipartimento di Fisica and NAST Centre Via della Ricerca Scientifica 1, Rome, 00133 Italy*

<sup>(4)</sup> *CNR-ISM, Area della Ricerca di Roma Tor Vergata - Via del Fosso del Cavaliere 100, 00133 Rome, Italy*

<sup>(5)</sup> *Centro Fermi, Museo Storico della Fisica e Centro Studi e Ricerche “Enrico Fermi” Piazza del Viminale 1, Rome, 00184 Italy*

<sup>(6)</sup> *CNR-IPCF Sezione di Messina - Viale Ferdinando Stagno d’Alcontres 37, Messina, 98158 Italy*

received 15 January 2021

**Summary.** — We apply the method of moment expansion, in terms of standard deviation and kurtosis, to the nuclear momentum and displacement distributions of hydrogen in biphenyl. In particular, we present first-principles calculations and we compare them to deep inelastic neutron scattering experiments, for the nuclear momentum distribution, and to X-ray diffraction, for the displacement distribution, so as to investigate the degree of anisotropy of the single-particle local potential. We find that, in the spirit of the central limit theorem, as a function of the increasing number of vibrations affecting a nucleus, the nuclear displacement distribution becomes more isotropic, as was the case of the nuclear momentum distribution, yet the trend is not monotonic with two local maxima at 125 meV and 20 meV.

### 1. – Introduction

Lignin is an organic polymer constituted of phenyl rings and its decomposition into monocyclic hydrocarbons is used for biofuel production [1]. Lignin has a complex and rigid structure that makes its degradation difficult, and it was suggested [2] that computational modelling of simpler compounds, such as biphenyl, could be used to research better ways for lignin treatment. First-principles phonon calculations, in the approximation of harmonic interaction potentials affecting nuclei within the molecule, are commonly used to simulate vibrational densities of states [3]. Recently we presented an investigation of the local hydrogen potential in biphenyl using Deep Inelastic Neutron Scattering (DINS) and first-principles computer simulations [4]. DINS [5] is an experimental technique accessing the Nuclear Momentum Distribution (NMD) in condensed matter systems. In particular, we showed that, experimentally, the effective potential affecting hydrogen in biphenyl was both harmonic and isotropic. In fact, as discussed by Sears [6], when the number of degrees of freedom in a given system increases, the three-dimensional NMD becomes a purely Gaussian function as a consequence of the Central Limit Theorem

(CLT). However, the experimental result was only partially reproduced in the phonon calculations because of the missing degrees of freedom arising from the structural disorder, mode couplings, and anharmonic effects. In this work we extend the formalism introduced in ref. [4] so as to take into account the degree of anisotropy of the Nuclear Displacement Distribution, NDD, at the same time as the one of the NMD. This is done analysing the kurtosis of both distributions, a measure of the deviation from a purely Gaussian function. In the framework of the CLT, we study the evolution of the NMD and NDD as functions of the increasing number of vibrations within the molecule.

## 2. – Materials and methods

The NMD and NDD of atom  $j$  within a 3D harmonic system can be expressed as

$$(1) \quad n(x_j) = \left\langle \prod_{\alpha} \frac{1}{\sqrt{2\pi}d_{j\alpha}} \exp\left(-\frac{x_{j\alpha}^2}{2d_{j\alpha}^2}\right) \right\rangle_{\Omega},$$

where  $\langle \dots \rangle_{\Omega}$  is the spherical average,  $x_{j\alpha}$  is the component along the Cartesian direction  $\alpha$  of either the momentum,  $\vec{x} = \vec{p}$ , in wave vector units, or displacement,  $\vec{x} = \vec{u}$ . Moreover,  $d_{j\alpha}^2$  is the standard deviation of the resulting multivariate distribution along  $\alpha$ , corresponding to either the mean square momentum,  $\sigma_{j\alpha}^2$ , or mean square displacement,  $\langle u^2 \rangle_{j\alpha}$ , respectively. The kurtosis of the distribution quantifies the degree of anisotropy of the multivariate distribution, and is defined as  $K[d_j^2] = \sum_{\alpha} d_{j\alpha}^4 / (\sum_{\alpha} d_{j\alpha}^2)^2$ , ranging between 1/3 for a completely isotropic system ( $d_{jx}^2 = d_{jy}^2 = d_{jz}^2$ ), to 1 for a highly anisotropic one. First-principles phonon calculations have been performed within Quantum Espresso [7] to compare with the experimental results from a biphenyl sample. For a general molecule with  $N$  nuclei and  $N_v = 3N$  vibrations, the dynamics is calculated from the dynamical matrix eigenvectors,  $\vec{e}_{vj}$ , and the eigenfrequencies,  $\omega_v$ , used to obtain the Vibrational Density of States (VDoS) [5], namely

$$(2) \quad g(\omega)_{j\alpha} = \sum_{v=1}^{N_v} \delta(\omega - \omega_v) e_{vj\alpha}^2 \quad \text{with} \quad \sum_{\alpha} \sum_{j=1}^N e_{vj\alpha}^2 = 1,$$

here  $e_{vj\alpha}^2 = |\hat{\alpha} \cdot \vec{e}_{v,j}|^2$  represents the contribution of the  $j$ -nucleus to the  $v$ -vibration in the  $\alpha$ -direction. The VDoS can be used to obtain the mean square momentum,  $\sigma_{j\alpha}^2$ , of the NMD and the mean square displacement,  $\langle u^2 \rangle_{j\alpha}$ , of the NDD, as

$$(3) \quad \sigma_{j\alpha}^2 = \sum_{v=1}^{N_v} \frac{\omega_v M_j}{2\hbar} e_{vj\alpha}^2 \coth\left(\frac{\hbar\omega_v}{2k_B T}\right); \quad \langle u^2 \rangle_{j\alpha} = \sum_{v=1}^{N_v} \frac{\hbar}{2M_j\omega_v} e_{vj\alpha}^2 \coth\left(\frac{\hbar\omega_v}{2k_B T}\right),$$

where  $k_B$  is the Boltzmann constant and  $T$  the temperature. Following the usual notation in the literature, we finally define  $\sigma_j^2 = (\sum_{\alpha} \sigma_{j\alpha}^2)/3$  and  $\langle u_j^2 \rangle = \sum_{\alpha} \langle u_{j\alpha}^2 \rangle$ , thus as the average and sum of the directional contributions, respectively.

## 3. – Results

Table I reports the experimental and calculated values of  $\sigma^2$  and  $\langle u^2 \rangle$  for hydrogen in biphenyl, as well as the values of the kurtosis of the NMD,  $K[\sigma^2]$ , and NDD,  $K[\langle u^2 \rangle]$ . In particular, the results are taken from ref. [4] for the NMD and from ref. [8] for the NDD. The newly calculated values of the kurtosis and  $\langle u^2 \rangle$  are reported in bold. The

TABLE I. – *Experimental and calculated result for the hydrogen NMD and NDD at 300 K.*

	$\sigma^2/\text{\AA}^{-2}$	$\langle u^2 \rangle / \text{\AA}^2$	$K[\sigma^2]$	$K[\langle u^2 \rangle]$
Experiment	$23.4 \pm 0.1$ [4] (DINS)	0.145 [8] (XRD)	$\simeq 1/3$ [4] (DINS)	0.36 [8] (XRD)
Simulation	24.6 [4]	<b>0.174</b> ; 0.185 [8]	<b>0.43</b>	<b>0.49</b>

experimental NMD was probed by a DINS experiment [4] on the VESUVIO spectrometer at the ISIS pulsed neutron source on a 0.5-mm-thick biphenyl powder sample, while the NDD was experimentally accessed by X-Ray Diffraction (XRD) analysis [8]. We discussed in ref. [4] the discrepancy in the degree of isotropy of the NMD by analysing the experimental and calculated dominating coefficient in the Gauss-Hermite expansion of the neutron Compton profile [9]. Here we adopt the more general value of the Kurtosis, for it can be directly applied to the NDD as well. Our calculated value of  $\langle u^2 \rangle$  is in relatively good agreement with the theoretical value and slightly larger than the experimental results both reported in ref. [8]. However, it should be noted that those experimental values had been provided for the average molecule using XRD measurements, and a better comparison can be obtained considering the mean square displacement of carbon, from our simulation, corresponding to  $0.065 \text{\AA}^2$ . We suggest that the difference between the experimental and simulated values of the kurtosis is even affected by model limitations where a real, powder sample is replaced by the perfect single crystal of the simulation without the inclusion of coupling effects between intra- and inter-molecular vibrations.

Equations (3) were used to evaluate the “running” values of the NMD and NDD kurtosis as a function of the increasing number of internal vibrations of biphenyl,  $N_v$ , starting from the highest energy stretching,  $\hbar\omega_M \sim 395 \text{ meV}$ . In particular, in fig. 1 we show the value of the kurtosis as a function of a lower limit of integration,  $\tilde{\omega}$ , such that, to calculate the corresponding value of  $K$ , only the frequencies in the range  $[\tilde{\omega}, \omega_M]$  were used. We showed how, in the framework of the CLT [6], the running kurtosis of the NMD was monotonically decreasing as the number of vibrations was increasing. When looking at fig. 1, while the value of the kurtosis of the NDD generally decreases, there

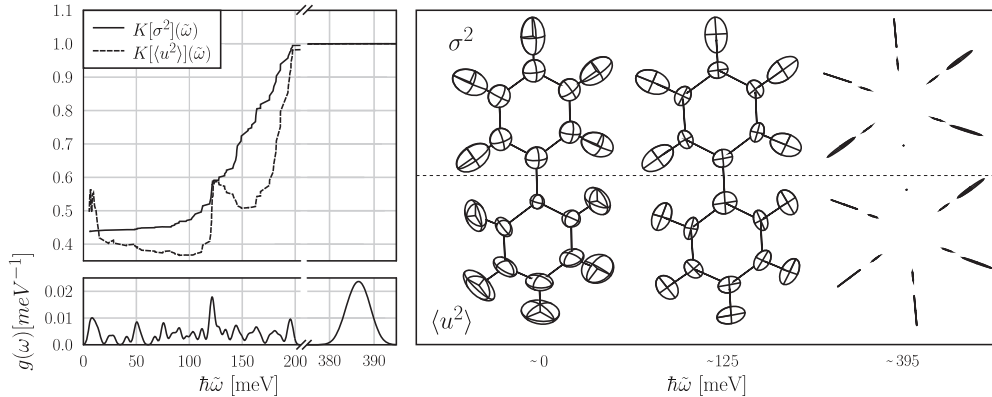


Fig. 1. – Hydrogen momentum and displacement kurtosis (left), thermal and kinetic ellipsoids (right) as a function of  $\tilde{\omega}$ , displayed using the ORTEP software.

are two regions where this is not the case. First, for  $\hbar\tilde{\omega} \simeq 125$  meV, where  $K$  has a local maximum. Looking at the right panel in fig. 1, one can appreciate that, changing  $\hbar\tilde{\omega}$  from the maximum value of 395 meV to the lower value of 125 meV, the shape of the NDD changes from a stick-like distribution, when only stretching modes are considered, to a disk-like distribution, when other planar vibrations are considered. The overall anisotropy of the NDD first decreases till the disk is a circle, then starts to increase again when the circle becomes an elliptic disc in the direction perpendicular to that of the original stick. When  $\tilde{\omega}$  is further decreased, the bidimensional disk changes to an ellipsoid, thus decreasing the value of the kurtosis, as out-of-plane vibrations are finally included. The final value of the kurtosis, *i.e.*, the actual degree of anisotropy, is however mainly defined by the low-energy vibrations, below 20 meV.

Finally, it is important to point out that the orientation of both the NMD and NDD ellipsoids change as a function of  $\tilde{\omega}$ , and the orientation is atom-dependent and in general it cannot be expressed in a common frame of reference, as was done for the simpler case of the water molecule in ref. [10].

#### 4. – Conclusion

We presented an investigation of the anisotropy of the hydrogen NMD and NDD using the novel idea of the running kurtosis. Our results can be explained in the framework of the CLT, whereby the local potential becomes more isotropic as the number of vibrations in the system increases. However, in the case of the NDD, two tendency inversions are observed, when the low-energy in-plane vibrations are added to the stretching modes, then when the low-energy out-of-plane deformations are also included. While the formalism is discussed in the case of biphenyl, it can be easily applied to other systems.

\* \* \*

The authors gratefully acknowledge the financial support of Regione Lazio (IR approved by Giunta Regionale n. G10795, 7 August 2019 published by BURL n. 69, 27 August 2019), ISIS@MACH (I), and ISIS Neutron and Muon Source (UK) of Science and Technology Facilities Council (STFC); the financial support of Consiglio Nazionale delle Ricerche within CNR-STFC Agreement 2014-2020 (N 3420), concerning collaboration in scientific research at the ISIS Neutron and Muon Source (UK) of Science and Technology Facilities Council (STFC) is gratefully acknowledged.

#### REFERENCES

- [1] RAGAUSKAS A. J., BECKHAM G. T., BIDDY M. J. *et al.*, *Science*, **344** (2014) 1246843.
- [2] DONG L., LIN L., HAN X., SI X., LIU X., GUO Y., LU F. *et al.*, *Chem*, **5** (2019) 1521.
- [3] TOGO A. and TANAKA I., *Scr. Mater.*, **108** (2015) 1.
- [4] ULPIANI P., ROMANELLI G., ONORATI D. *et al.*, *J. Chem. Phys.*, **153** (2020) 234306.
- [5] ANDREANI C., KRZYSTYNIAK M., ROMANELLI G. *et al.*, *Adv. Phys.*, **66** (2017) 1.
- [6] SEARS V. F., *Can. J. Phys.*, **63** (1985) 68.
- [7] GIANNOZZI P., BARONI S., BONINI N. *et al.*, *J. Phys: Condens. Matter.*, **21** (2009) 395502.
- [8] BONADEO H. T. and BURGOS E., *Acta Cryst. A*, **38** (1982) 29.
- [9] ROMANELLI G. and KRZYSTYNIAK M., *Nucl. Instrum. Methods A*, **819** (2016) 84.
- [10] FINKELSTEIN Y., MOREH R., BIANCHINI F. *et al.*, *Surf. Sci.*, **679** (2019) 174.